Palaeogeography, Palaeoclimatology, Palaeoecology 560 (2020) 110041

Contents lists available at ScienceDirect

Palaeogeography, Palaeoclimatology, Palaeoecology

journal homepage: www.elsevier.com/locate/palaeo

Invited Research Papers

Sediment dynamics of estuarine Holocene incised-valley fill deposits recorded by *Siphonichnus* (ancient Red River, Gulf of Tonkin)

Andreas Wetzel[a,*], Daniel Unverricht[b]

[a] Department of Environmental Sciences – Geology, University of Basel, CH-4056 Basel, Switzerland
[b] Institut für Geowissenschaften, Christian-Albrechts-Universität, Otto-Hahn-Platz 1, D-24118 Kiel, Germany

ARTICLE INFO

Keywords:
Ichnology
Equilibrichnia
Fluvio-marine transition
Open estuary
Deposition
Erosion

ABSTRACT

The Holocene muddy infill of the valley incised by the ancient Red River during Pleistocene sea-level lowstand records a change from fluvial to estuarine and finally marine depositional conditions. *Siphonichnus*, a mainly vertical trace fossil produced by burrowing bivalves, documents otherwise unrecorded episodes of enhanced erosion, bypass and deposition of, on average, rapidly aggrading (> 1 m kyr^{-1}), mainly completely bioturbated sediments within the fluvial-marine transition zone (FMTZ), supposedly within the polyhaline domain. The producers of *Siphonichnus* moved nearly 1 m downward or upward in response to erosional or depositional phases, respectively. The fill of *Siphonichnus* burrows, in addition, records erosion and/or bypass of sediment: The traces were produced in mud, but many of them are filled with coarse silt and sand that is otherwise not present in the studied intervals in distinct layers. Obviously, this material was available when *Siphonichnus* was produced and connected to the sediment surface. In addition to seasonal erosion and deposition during freshet and its waning stage, *Siphonichnus* records exceptional events that displace the sediment surface by > 0.5 m. Such events occurred episodically at an estimated frequency of 1 event per several hundreds of years. The complete bioturbation of the deposits suggests apparent continuous accumulation, but in fact they represent a pile of stacked event deposits resulting from depositional phases and intermittent severe erosion.

1. Introduction

During times of considerably lowered sea level, rivers incised valleys into exposed shelf areas (e.g., Zaitlin et al., 1994; Boyd et al., 2006). During the Quaternary, sea-level fall was so rapid that rivers did not reach geomorphic equilibrium and hence, remained in a potentially erosional mode (e.g., Schumm, 1993; Fagherazzi et al., 2004). Consequently, deposition of fluvial sediments was normally low. The situation changed when a river segment became affected by sea-level rise and switched to an aggrading mode within the fluvial-marine transition zone [FMTZ] (e.g., Zaitlin et al., 1994; Boyd et al., 2006). The valley fill provides a rather complete record of the transgression compared to adjacent areas (e.g., Mattheus and Rodriguez, 2011).

For organisms, the FMTZ represents a demanding habitat because environmental conditions fluctuate severely (e.g., Howard and Frey, 1975; Gingras et al., 2012; La Croix et al., 2015). These fluctuations are rather pronounced when the catchment area experiences a seasonal climate and, hence, river discharge considerably varies (e.g., Dashtgard and La Croix, 2015; Gugliotta et al., 2017). In addition, mud aggregating along the saltwater-freshwater contact may lead to the (temporary) presence of a fluid-mud carpet of condsiderable thickness (e.g., Franz et al., 2014; Azhikodan and Yokoyama, 2018). In response to runoff, erosional and depositional phases alternate during onset and waning freshet as seawater intrusion does, reaching furthest upstream during times of low discharge. Even if salinity can be reliably measured, in many instances species typical of a distinct salinity imply a further upstream extent of seawater wedge than hydrochemical data do (e.g., Gugliotta et al., 2017). For example, in the Mekong River, chemical data indicate an upstream extent of saline water for 50 km during dry season, whereas a brackish fauna occurs up to 160 km inland the river mouth (Gugliotta et al., 2017) that, however, can also be seen as a function of larval recruitment (e.g., Gingras et al., 2012). The record of such hydraulic processes by physical sedimentary structures is limited (see La Croix and Dashtgard, 2015) and this is particular true in the Holocene fill of the Red River incised valley that is completely mud dominated and strongly bioturbated (Wetzel et al., 2017; see below). Furthermore, the considerable organic matter content of estuarine deposits favors the dissolution of calcareous shells (e.g., Aller, 1994). Therefore, bioturbational structures document the environmental situation better than shells because traces reflect the general adaptation

* Corresponding author.
E-mail addresses: andreas.wetzel@unibas.ch (A. Wetzel), daniel.unverricht@ifg.uni-kiel.de (D. Unverricht).

https://doi.org/10.1016/j.palaeo.2020.110041
Received 11 March 2020; Received in revised form 17 September 2020; Accepted 19 September 2020
Available online 28 September 2020

of an organism to its biotope and they are autochthonous and cannot become displaced or dissolved (e.g., Hertweck, 1972; Goldring, 1995).

The trace *Siphonichnus* occurs in marine deposits but also in estuarine, brackish, and even freshwater settings (Knaust, 2015). It is produced by bivalves that burrow downward or upward in response to erosion or deposition, respectively (e.g., Reineck, 1958; Stanistreet et al., 1980). Direction of movement is indicated by the fill of the trace (for details see below). Traces recording the response of their producers to erosion or deposition are called equilibrichnia (e.g., Bromley, 1996). Most of the knowledge about the trace fossil *Siphonichnus* and its environmental significance relies on findings in the rock record (see review by Knaust, 2015 and references therein). In contrast, there is no detailed study of this ichnogenus in modern sediments for which the environmental conditions are fairly well known.

The Holocene sediments filling the valley system incised by the Red River and its tributaries into the Gulf of Tonkin area during sea-level lowstand commonly contain *Siphonichnus*. The Red River represents such an 'out-of-equilibrium' fluvial system (see above) located in an area subjected to pronounced climatic seasonality and hence, experienced strongly fluctuating environmental conditions (Wetzel et al., 2017). It is the purpose of the present paper, (i) to describe the morphology and geometry of *Siphonichnus* traces, (ii) to show so far not observed morphologic variants and modifications, (iii) to relate their occurrence to the fairly well known environmental conditions, (iv) to demonstrate their potential to indicate otherwise not recorded sediment dynamics, and (v) to demonstrate the environmental significance of these burrows in combination with additional sedimentary features.

2. Study area and geological background

The Gulf of Tonkin forms an extensive shelf area in the NW part of the East Sea (South China Sea) (Fig. 1). The monsoon system affects the entire region (e.g., Tomczak and Godfrey, 1994). Two different monsoonal regimes acted during the Quaternary (e.g., Wang et al., 1999; Wang and Li, 2009). Interglacial times as today are characterized by weak NE monsoon and weak seasonality. During May to September, the strong SW monsoon provides humidity and leads to a wet season in the SE Asian mainland, whereas during November to March, the monsoon reverses and results in a dry season (Wang et al., 1999; Wang and Li, 2009). Glacial times are characterized by strong NE monsoon during winter and weak SW monsoon during summer and low wetness in subtropical China (e.g., Wang et al., 1999; Liu et al., 2007). Therefore, fluvial runoff to the northern part of the East Sea decreased (Wang et al., 1999). During glacial times, when sea level was lowered by > 100 m, wide shelf areas were exposed and drained by several rivers (e.g., Voris, 2000).

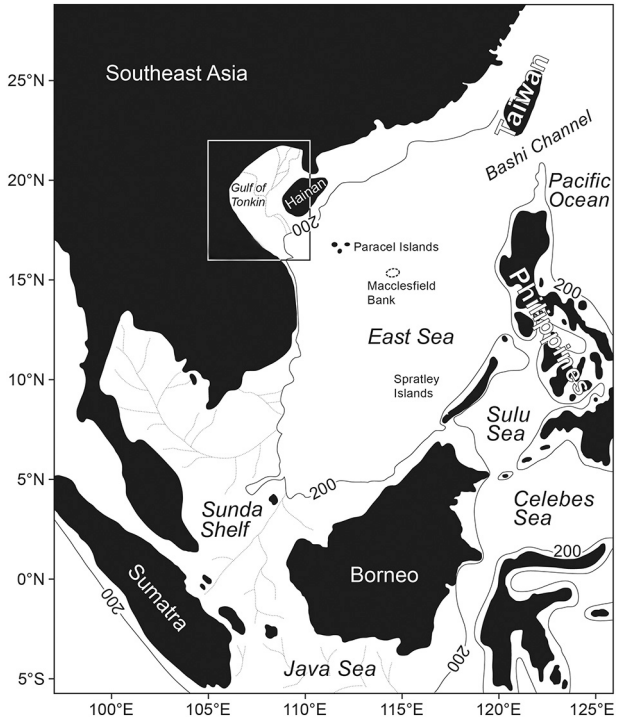

Fig. 1. East Sea (previously South China Sea) and location of the study area (frame, shown in Fig. 2).

After the Last Glacial Maximum, inundation of the exposed shelf areas started around 19.6 ka (Hanebuth et al., 2009) and continued until the mid-Holocene sea-level maximum at ~6 ka (Stattegger et al., 2013). Sea-level rise and the concomitant rise of local base level resulted in sediment aggradation in incised valleys and transformed them into estuaries (e.g., Hanebuth and Stattegger, 2003; Tjallingii et al., 2010). Because of pure geometrical reasons a pronounced sea-level rise affecting a low-gradient coastal area leads to rapid transgression of the shoreline. Thin, transgressive shoreface sediments accumulated outside the incised valleys and Holocene marine deposits rest on Pleistocene sediments separated by a rather sharp boundary (e.g., Schimanski and Stattegger, 2005; Szczuciński et al., 2013).

The Gulf of Tonkin occupies an area of 90,000 km^2; the island of Hainan borders it to the east and the Asian mainland to the north and the west (Fig. 2). The Gulf of Tonkin experiences diurnal tides, with a tidal range of 4 m in the north and 2 m in the south (van Maren, 2007).

The Red River originates in the mountainous area of Yunnan and drains an area of about 168,000 km^2 (Haruyama, 1995). The mean annual discharge is around 3810 m^3 s^{-1} (= 120 km^3 yr^{-1}), but it fluctuates between 23,000 and 700 m^3 s^{-1} from the wet to the dry

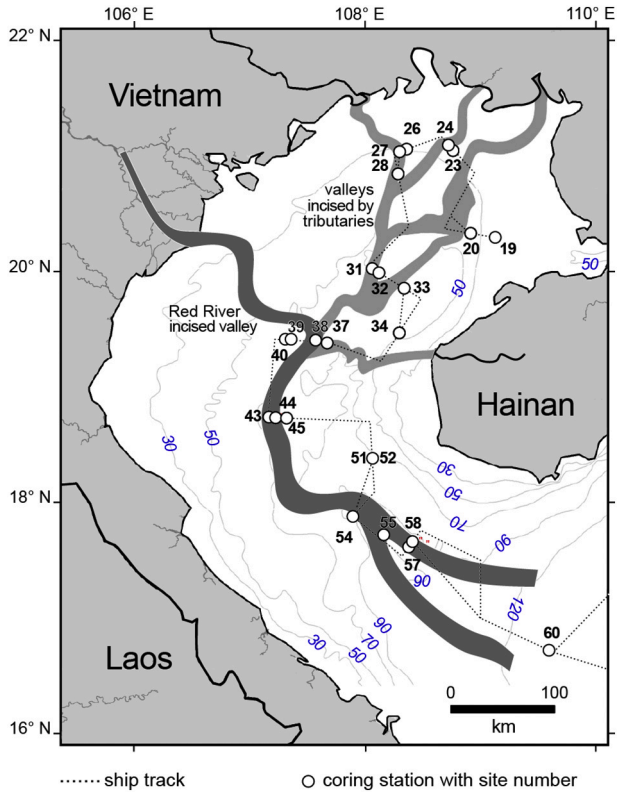

Fig. 2. Gulf of Tonkin and the valley system incised during pre-Holocene sea-level lowstand by the ancient Red River and its tributaries; inland parts of valleys formed prior to late Holocene coastline progradation (Tanabe et al., 2006). Depth contour lines in metres (depth values in blue italic numbers) and core stations (bold numbers). (For interpretation of the references to colour in this figure legend, the reader is referred to the web version of this article.)

season (Mathers and Zalasiewicz, 1999). The river carries about 123 Mt. yr^{-1} suspended load and 10 Mt. yr^{-1} bed load; about 90% of the annual suspended sediment load is tranferred during the summer monsoon season (Mathers and Zalasiewicz, 1999; Borges and Huh, 2007). Although the discharge of the Red River significantly decreased during glacial times, a well-developed valley system was incised into the substrate (Fig. 2; Wetzel et al., 2017). During the middle Holocene, the sediment discharge was about one-third of its present-day value (Tanabe et al., 2006). The Red River traverses an approximately 200-km wide coastal plain before reaching the modern delta and, during times of lowered sea level, it formed a piedmont incised valley sensu Zaitlin et al. (1994).

The infill of the valley incised by the ancient Red River was studied in detail by Wetzel et al. (2017): The Gulf of Tonkin coastline migrated at an average rate of ~60 m yr^{-1} landward during Holocene sea-level rise (20–8 ka). Due to a combination of rapid coastline migration and undersupply of sand neither coastal barriers nor tidal sand bars developed at the mouth of the Red River incised valley. Only a 30–80 cm thick muddy sand interval is preserved at the base of fully marine deposits. Thus, the river mouth represented a mud-dominated, open, funnel-shaped estuary during transgression that favored upstream incursion of seawater. The estuarine deposits aggraded on average rapidly, up to a few meters per kyr as expressed in seismic records by stacked reflectors (Fig. 3).

The cores taken from the Holocene fill of the valley incised by the ancient Red River show a rather similar succession and are attributed to five lithofacies (LF; Wetzel et al., 2017; Figs. 4, 5). Lithofacies 1 (LF1) comprises greenish gray, muddy coarse-sandy to pebbly sediment containing mud clasts, carbonate and Fe-oxide nodules (Fig. 4a). LF1 typically occurs directly above indurated Pleistocene mud and is interpreted to represent fluvial lag deposits. The discontinuity at the base fulfils some, but not all criteria of a sequence boundary (SB; see discussion by Blum et al., 2013; Fig. 5). LF1 comprises the lowstand systems tract (LST) and its top is also the top of LF1, limited by the transgressive surface (ts) (Fig. 5).

Above the ts, greenish gray mud accumulated. Upwards within this unit, degree of bioturbation and size of burrows increases, the amount of early diagenetic siderite nodules decreases, and the frequency of thread-like Fe-sulfide precipitates increases. This muddy unit comprises two endmembers; (1) laminated mud (LF2) exhibiting millimetric laminae and occasionally centimetric uniform mud layers, and (2) totally bioturbated beds (LF3; Fig. 4c). LF2 dominates the lower part of the muddy succession above the ts but further up, a few centimeters thick intervals of LF3 are increasingly intercalated until LF3 dominates. The entire mud unit formed in the FMTZ (Wetzel et al., 2017). Laminated mud containing early diagenetic siderite indicates fluvial dominance, whereas the bioturbated estuarine mud containing Fe-sulfides was considerably affected by seawater (cf. Postma, 1982). This interval ends where the sand content significantly increases.

Lithofacies 4 (LF4) comprises greenish to pale, 30–80 cm thick, completely bioturbated, poorly sorted fine to coarse sand containing a considerable proportion of mud and (debris of) marine shells. LF4 records the onset of full marine conditions. The marine transgressive surface (mts) is not well developed because of intense bioturbation and some deep-reaching burrows containing sand displaced downward into LF3. Therefore, the mts is placed where the sandy interval is laterally continuous (Fig. 5; Wetzel et al., 2017). Further up, the sand content decreases and is replaced by mud.

In fresh core, visually uniform to slightly mottled greenish mud (LF5) contains (debris of) marine shells and microfossils and appears completely bioturbated in X-ray radiographs. LF5 represents fully marine deposits. The maximum flooding surface (mfs; Fig. 5) is not recognizable because of uniform grain-size composition and complete bioturbation.

3. Material and methods

The present study is based on 21, 12-cm diameter gravity cores up to 10 m long and 21, 50·50 cm^2 box cores up to 40 cm long taken along seismic transects (Fig. 2; Table 1). The cores were retrieved during cruise 220 of the German research vessel *Sonne* in 2012 to the East Sea (Wiesner et al., 2012). The Holocene valley fill sequence was not

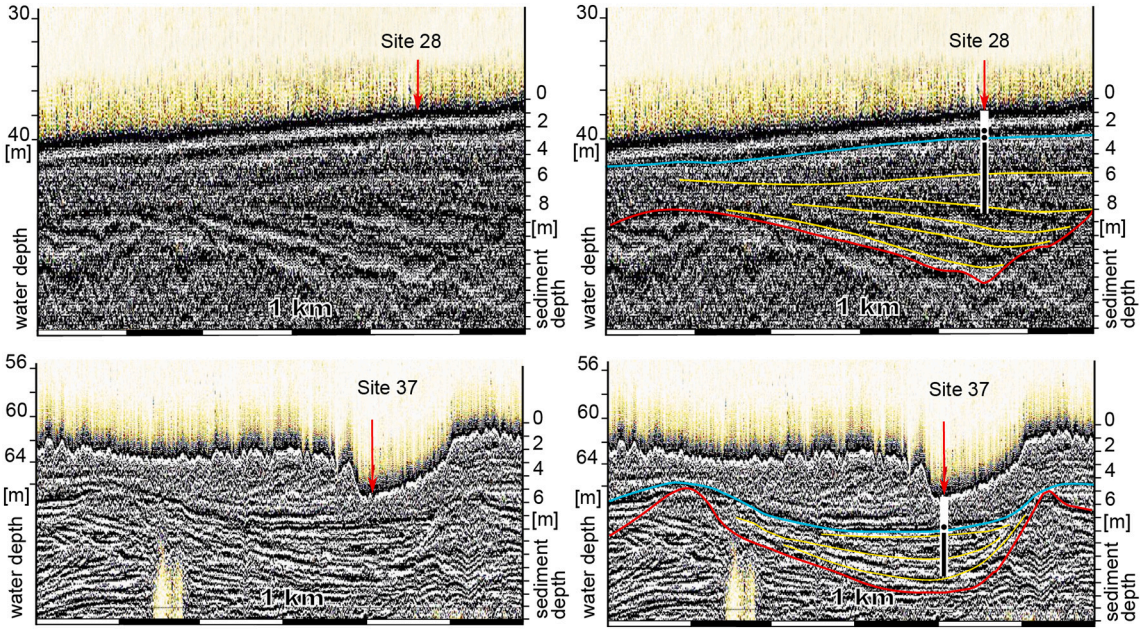

Fig. 3. Seismic sections showing the Holocene fill of the valley systems incised by the Red River and its tributaries during times of lowered sea level. Numbers refer to sites shown in Fig. 2. Two versions of each line are shown including the uninterpreted (left) and interpreted (right) lines and lithofacies encountered in core (White – LF 5, black dot – LF 4, black bar – LF 2/3 as outlined in text). The unconformity at the base (red line) represents a sequence boundary overlain by lag deposits only a few (tens of) centimeters thick corresponding to the Lowstand Systems Tract; the Transgressive Systems Tract is characterized by a set of aggrading reflectors (yellow lines) that formed during rapid sea-level rise bounded by the marine transgressive surface (mts) that is covered by rather uniform marine mud continuing up to the modern seafloor. (For interpretation of the references to colour in this figure legend, the reader is referred to the web version of this article.)

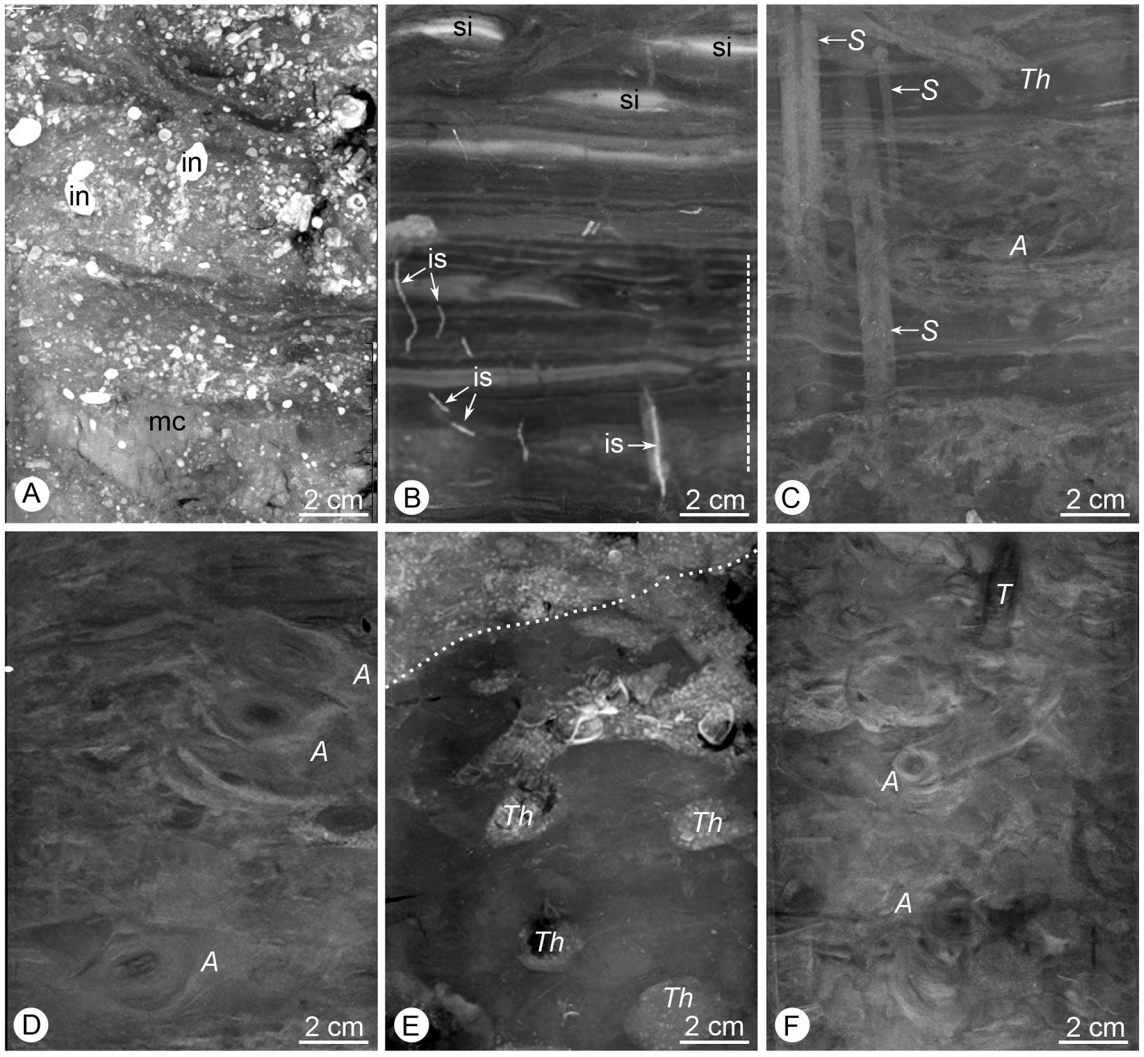

Fig. 4. Examples of lithofacies (LF) in X-ray radiographs (sand – light, mud – dark). (A) LF 1 – Fluvial lag deposits exhibiting coarse texture, presence of mud clasts (mc), and iron oxide nodules (in) (core 55–5, 76–90 cm). (B) LF 2 – Laminated fluvial mud composed of silt/fine-sand layers and mud; thick event layer marked by broken line; conditions fluctuating between dominance of fluvial and marine water are indicated by the presence of both siderite (si) and iron sulfides (is) (core 54–1, 331–344 cm). (C) LF 2/3 – Alternating intervals consisting of bioturbated and laminated mud; *S* = *Siphonichnus* (note the small size), *A* = *Artichnus*, *Th* = *Thalassinoides* (core 58–2, 325–338 cm). (D) LF 3 – Completely bioturbated estuarine mud, *A* = *Artichnus* (probably produced by holothurians or sipunculids, indicating > 20–25 PSU or > 15 PSU, respectively) (core 52–2, 283–297 cm). (E) LF 4 – Bioturbated sand deposited above the marine transgressive surface (mts) marked by stippled line; coarse marine material was displaced by producers of *Thalassinoides* (*Th*) (core 57–5, 2–26 cm). (F) LF 5 – Bioturbated marine mud; *A* = *Artichnus*; *T* = *Teichichnus* (core 19–28, 26–40 cm).

completely cored in the center of the main valley, only at its margins.

Descriptions of all cores are based on onboard visual observations, digital camera images, and X-ray radiographs, which show sedimentary structures of soft muddy sediments in far more detail than fresh core (e.g., Wetzel, 1981, 2010). For X-ray radiography, about 1 cm thick sediment slabs were taken from the split core surface directly after opening and sealed to prevent desiccation (Werner, 1967). The slabs were irradiated at the Radiology Section of the Medical Care Center (Prüner Gang) in Kiel (Germany) using a Swissray ddR Multi System operated at 40 kV and 100 mAs and automatically controlled radiation time. Because burrows in the slabs were analyzed, their 3D geometry and ornamentation are unknown and therefore, the taxonomic evaluation of the burrows is restricted to the ichnogenus level (e.g., Gerard and Bromley, 2008; Knaust, 2017). The taxonomic affinity was evaluated by the geometric approach suggested by Knaust (2012) using those ichnotaxobases of Bertling et al. (2006) that are seen in X-ray radiographs: orientation of a burrow, presence or absence of branching, shape, presence or absence of lining/mantle, and fill structure. Although this classification is subject to some error, a taxonomic classification should allow comparison between modern examples and their fossil counterparts. However, the taxonomic classification of burrows occurring in soft sediments has to be taken provisionally (e.g., Bertling et al., 2006). To estimate trace density a semi-quantitative approach was applied (e.g., Wetzel and Werner, 1981; Ayranci et al., 2014).

4. Observations

Within the FMTZ deposits of the Holocene incised valley fill, *Siphonichnus* is present in 9 of 21 cores taken in water depth ranging from 20 to 90 m, mainly at marginal positions of the valley-fill succession where seismic reflectors are nearly horizontal (Fig. 3). *Siphonichnus* was not observed in deposits formed at valley bends (Fig. 2). If present, *Siphonichnus* occurs in rather high abundance and appears to cluster: Within an interval 1–1.5 m below the marine transgressive surface, 8 *Siphonichnus* were encountered in 5 of 21 cores, each core having an undisturbed horizontal cross-sectional area of 100 cm^2 and thus, assuming a uniform distribution, on average, 40 specimens occur

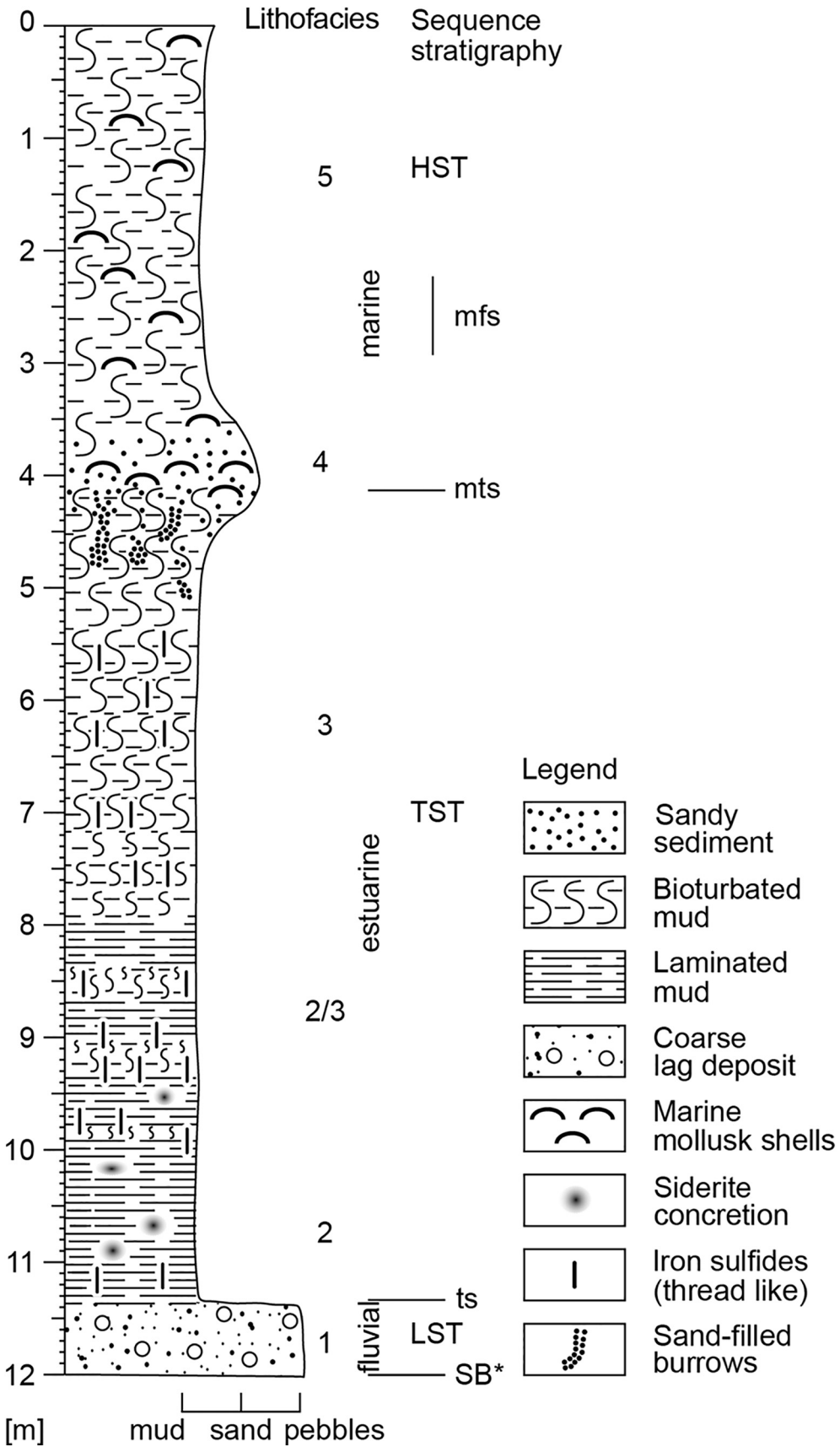

Fig. 5. Schematic, synthetic lithologic log of the mud-dominated deposits filling the valley incised by the ancient Red River in the Gulf of Tonkin. The thickness of the lithofacies may vary in response to valley gradient; here average values are shown (for details see text). Numbers referring to lithofacies types as explained in text and shown in Fig. 4. Sequence stratigraphic abbreviations; SB* = erosional unconformity not necessarily representing a true sequence boundary (see Blum et al., 2013), ts = transgressive surface, mts = marine transgressive surface, mfs = maximum flooding surface that in fact is not sharply defined, rather representing an interval; LST = lowstand systems tract; TST = transgressive systems tract; HST = highstand systems tract. (For interpretation of the references to colour in this figure legend, the reader is referred to the web version of this article.)

Table 1
Location of coring sites (from Wiesner et al., 2012).

Site	Latitude [N]	Longitude [E]	Water depth [m]
19	20°17.613′	109°08.266′	22
20[a]	20° 19,941′	108°55,093′	45
23[a]	21°05.838′	108°43.534′	27
24	21°06.694′	108°43.792′	26
26	21°03.421′	108°20.488′	28
27	21°02.518′	108°18.151′	32
28	20°49.763′	108°17.464′	40
31[a]	20°00.637′	108°05.476′	49
32	19°59.529′	108°07.444′	66
33	19°51.526′	108°20.382′	55
34	19°27.453′	108°17.587′	59
37	19°22.655′	107°41.945′	66
38	19°25.059′	107°34.341′	65
39	19°25.441′	107°21.333′	61
40	19°25.034′	107°18.047′	58
43	18°47.548′	107°09.967′	65
44	18°44.227′	107°11.764′	67
45	18°44.040′	107°16.236′	67
51	18°22.809′	108°03.829′	75
52	18°22.376′	108°03.873′	76
54	17°53.425′	107°54.124′	91
55[a]	17°41.959′	108°07.020	87
57	17°38.420′	108°23.869′	109
58	17°39.925′	108°24.997′	107
60	16°43.544′	109°35.360′	553

[a] At these sites, a thin Holocene muddy sand layer covers a Pleistocene paleosol.

per 1 m^2. This abundance estimate does not take in account that only a 10-cm wide, 1 cm-thick longitudinal section of the core was analyzed by X-ray radiography (covering one-tenth of the horizontal core cross-sectional area). Given the volume of a burrow having a circular cross-section and 3 cm diameter, about half of the core was unavailable for observation of *Siphonichnus*. Therefore, the abundance of burrows is supposedly higher than the above value of ~40 specimens per 1 m^2.

In 20 cm sediment depth, an articulated bivalve 0.9 cm in size was found in situ within a 1-cm wide *Siphonichnus* connected to the surface (Fig. 6). It matches previous findings that bivalves produce *Siphonichnus* (e.g., Stanistreet et al., 1980; Knaust, 2015). In the studied cores, *Siphonichnus* occurs in completely bioturbated marine (LF 4, LF5) and brackish-estuarine sediment (LF 3), and in partly bioturbated, otherwise laminated transitional sediment (LF 2/3), but it is absent in fluvial-dominated mud (LF2) and fluvial lag deposits (LF 1; Fig. 4; Wetzel et al., 2017). In the case of LF2/3, *Siphonichnus* cross-cuts LF2 but very likely originated from bioturbated intervals (LF3). *Siphonichnus* reaches its largest width and penetration depth in completely bioturbated sediments that formed when the estimated mean salinity clearly exceeded a threshold value indicated by the trace *Artichnus*. This trace is so far interpreted to be produced by holothurians and therefore, may characterize salinities estimated to be > 20 PSU (Wetzel et al., 2017) or 25–30 PSU (Ayranci and Dashtgard, 2013; see below: Discussion).

The studied *Siphonichnus* comprises J-shaped, straight to slightly curved or undulating burrows. It is nearly vertical (90° ± 15°) in the upper part and becomes inclined to supposedly horizontal within its deepest part where inclination approaches < 20° (0° = horizontal; Fig. 7). Due to its undulating course, *Siphonichnus* may disappear from the plane of observation given by the radiograph slab. There are two expressions of the *Siphonichnus* backfill depending on the direction of movement of the producer. Downward, the backfill exhibits (1) convex mensisci traversed by (2) a lumen (produced by the siphon) in the center, called (1) mantle and (2) core by Knaust (2015), for the latter term, however, in this study 'lumen' or 'siphonal lumen' is used instead (Fig. 7). When digging upward, the backfill consists of irregular, concave lamellae and the producer followed (partly) its own previously formed trace (Figs. 7, 8). The margin of the traces appears more sharply developed in a

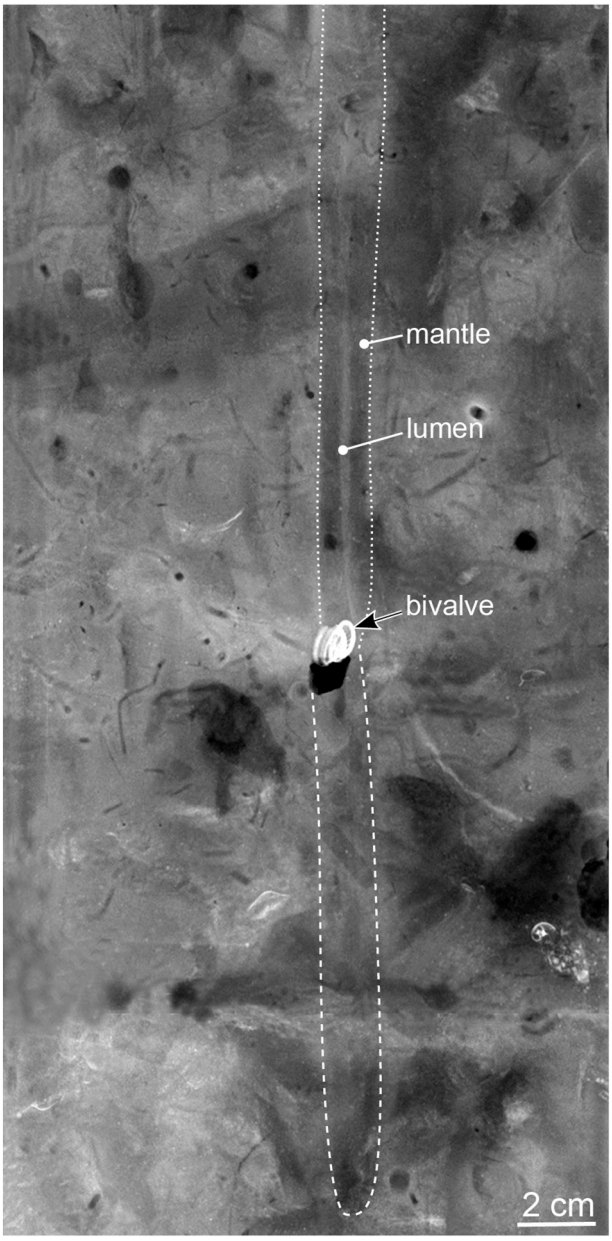

Fig. 6. Bivalve within *Siphonichnus* (core 42–2, 0–30 cm; X-ray radiograph; mud – dark, sand – light). Stippled line envelopes burrow part showing central lumen produced by siphon overprinting the fill menisci; dashed line below the bivalve (arrow) demarcates upward movement of the producer.

downward burrow segment than in an upward one (Fig. 7). Twenty-five downward and 20 upward burrow segments were observed. Around *Siphonichnus* burrows no compressional features are recognizable.

Siphonichnus commonly occurs in muddy host sediment. The mantle emplaced when moving downward exhibits rather regular convex menisci that are enriched in coarse silt and fine sand alternating with more muddy material. They are fairly straight and inclined at an angle of 30°–45° to the margin of the burrow, and they display a rather uniform spacing of ~3–5 mm (Figs. 7, 8). The lumen displays a uniform muddy or sandy fill; occasionally Fe-sulfides are present. The backfill emplaced when moving upward has an irregularly laminated, collapsed to fluidized appearance. The laminae extend downward for ~1–2 times of the burrow width and in the central part a tongue-like downward protrusion may occur. The laminae display an irregular spacing ranging from 1 to 15 mm, and occasionally thin laminae are arranged in packages of 2–5 (Fig. 7).

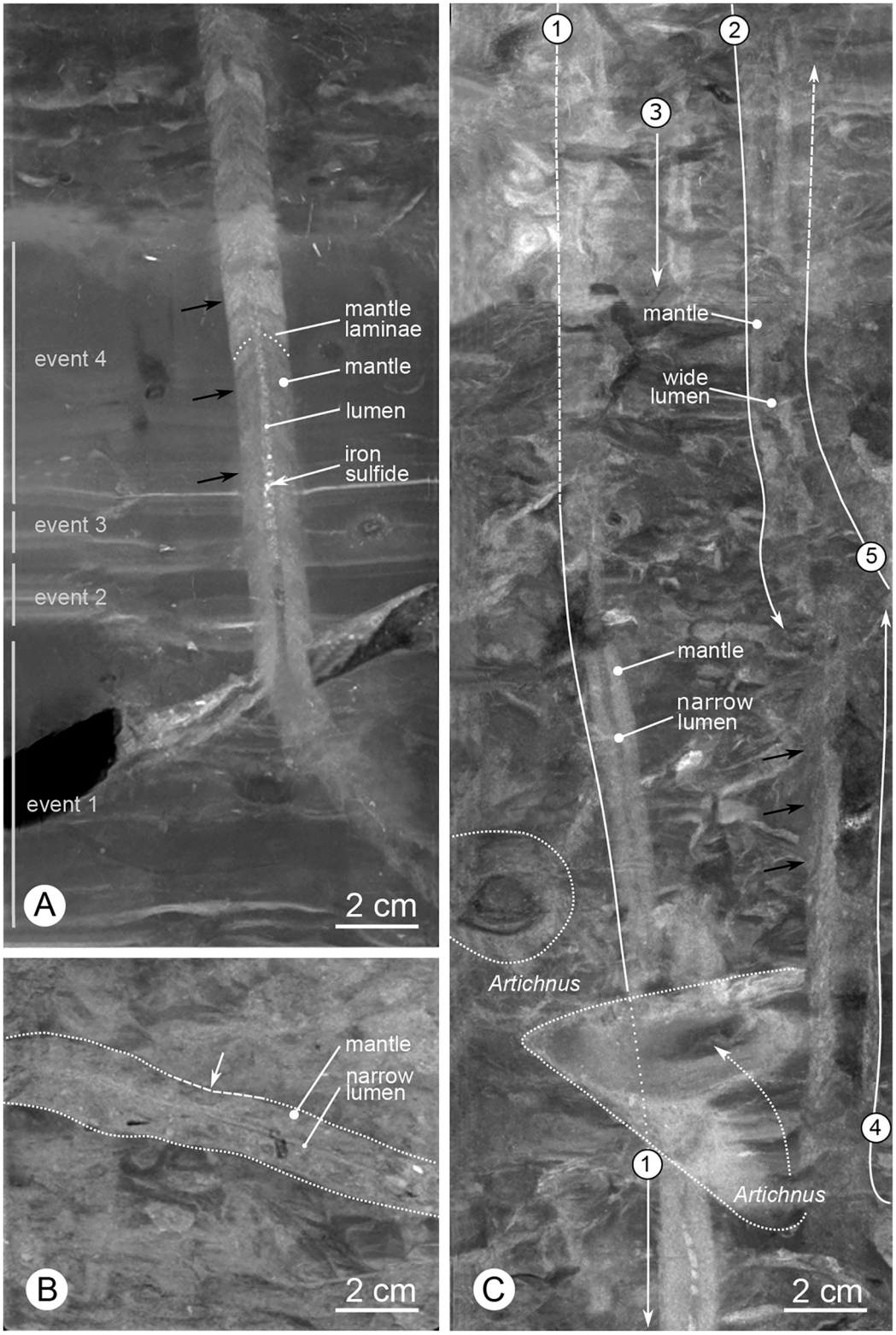

Fig. 7. Elements of *Siphonichnus*, in particular downward, upward and horizontal movements (X-ray radiograph negatives; mud – dark, sand – light). Location of cores is shown in Fig. 2. (A) Downward movement indicated by the (siphonal) lumen traversing a laminated inclined backfill (mantle) having a sharp margin (black arrows); backfill is coarser (lighter) than host sediment; iron sulfide (very light) is locally present in the lumen; graded mud packages represent depositional events (core 27–3; 370–390 cm). (B) Horizontal *Siphonichnus* (between stippled lines) indicating movement to the right; backfill is less systematically structured than in vertical specimens and the lumen is clearly developed; upper part of *Siphonichnus* overprinted by another burrow (marked by dashed line; white arrow) (core 28–4, 568–575 cm). (C) Cluster of *Siphonichnus,* each specimen and direction of movement marked by number and arrow; downward movement is characterized by laminated mantle cross-cut by the lumen (specimens 1–3), upward movement results in chaotic mantle and absence of a lumen (specimens 4, 5); note different width of lumina relative to total burrow width, narrow lumen: specimen 1, wide lumen: specimens 2, 3. *Artichnus* is characterized by eccentric spreite fill, its deep production is indicated by cross-cutting *Siphonichnus* specimens 1, 2 (core 26–5; 219–250 cm; 66 m water depth).

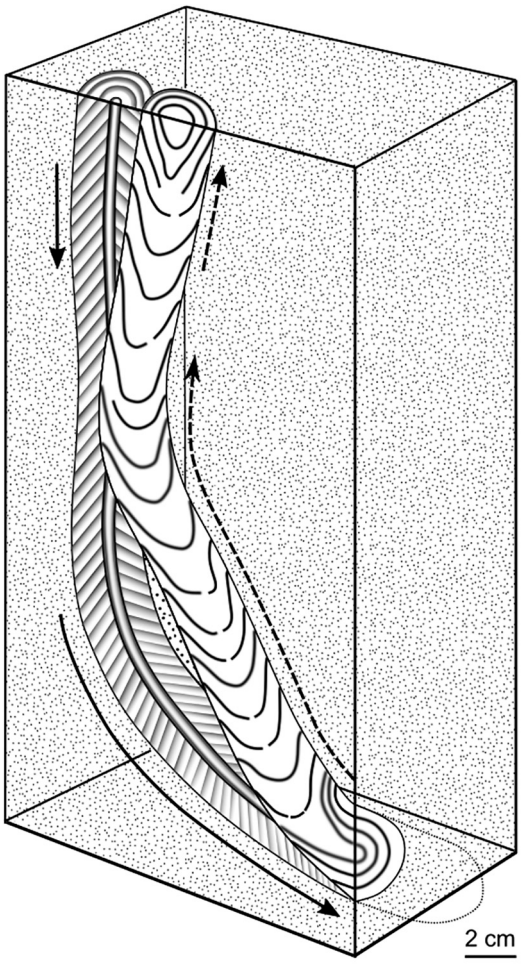

Fig. 8. Schematic drawing of the lower part of *Siphonichnus* encountered in the Holocene incised valley fill deposits in the Gulf of Tonkin showing structures formed during downward movement (mantle menisci cross-cut by the lumen) becoming increasingly inclined and finally horizontal (arrow), and upward movement (dashed arrow) exhibit chaotic wide-spaced lamination.

The observed *Siphonichnus* traces display a rather constant width along their course. Although burrow size varies in response to environmental conditions, two groups of *Siphonichnus* can be distinguished that differ in the ratio of burrow width (w_b) to width of siphonal lumen (w_s) being 2–5 and 6–9, respectively (Figs. 7, 9). The maximum width of *Siphonichnus* is 3.3 cm, the minimum 0.3 cm. In the early estuarine deposits, small burrows occur more frequently than further up (Wetzel et al., 2017). Penetration depth roughly correlates with burrow width: Downward, a 3-cm wide burrow may penetrate for up to 1 m and a 0.5-cm wide *Siphonichnus* only for 40–50 cm; correspondingly, upward movements of 90 cm and 40 cm have been observed (Fig. 10).

Due to clustering of burrows, in a few cores recurrent downward and upward movement is recorded for *Siphonichnus* producers of various size (Figs. 10, 11). *Siphonichnus* truncated by erosion has not been observed, but other burrows cross-cut *Siphonichnus*, for instance, *Artichnus*, *Taenidium*-like traces and irregularly backfilled burrows (Fig. 10).

5. Interpretation

Producers are only rarely encountered within *Siphonichnus* (Knaust, 2019, pers. comm.). The bivalve found in situ in a *Siphonichnus* connected to the surface probably died shortly before coring and the time

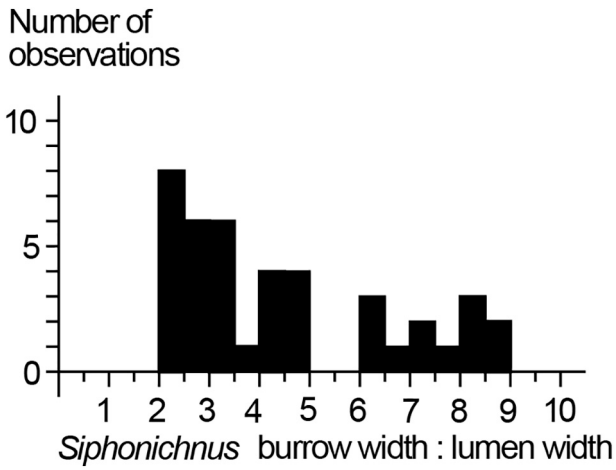

Fig. 9. *Siphonichnus* exhibiting two groups distinguished by the ratio of burrow width (w_b) versus lumen width (w_s) imply different groups of organisms (bivalves) producing the trace.

was too short to dissolve the shells. Commonly, after death of a bivalve, CO_2 produced by oxic oxidation of organic matter facilitates carbonate dissolution (e.g., Aller, 1994). The bivalve found in-situ provides information about the living depth of *Siphonichnus* producers; it increases with body size. A burrowing depth in the range of 15 cm, 20 cm, and 30–40 cm are, thus, deduced for bivalves having 0.5 cm, 1.0 cm, and 3 cm body size, respectively. The first and last values rely on observations of downward and upward burrow segments. However, the observed trend of increasing burrowing depth with increasing body size does not apply for bivalves generally because some adult bivalves, for instance *Mya arenaria*, cannot readjust their burrows (e.g., Kranz, 1974; Dashtgard and Gingras, 2012).

The abundance of > 40 specimens per 1 m^2 does not reflect the population density of *Siphonichnus* producers, which can hardly be estimated because erosion very likely removed parts of burrows and other organisms have overprinted shallow segments of *Siphonichnus*. Furthermore, a *Siphonichnus* producer that penetrated 50 cm deep moved through an interval representing about 500 years at a sedimentation rate of 1 m kyr^{-1}, but the (unknown) life span is probably in the range of 3–10 years as for other marine bivalves (e.g., Moss et al., 2016). The latter aspect causes an overestimation of the producers' abundance in the sediment record.

The rather constant width of *Siphonichnus* implies that the producer moved repeatedly downward and upward and enlarged the burrow during growth. New burrows were probably not formed during subsequent growth stages. To do so, a young, small bivalve needs to move upward to abandon its burrow and to start a new one elsewhere. Therefore, there should be numerous smaller traces showing only upward movement within the same interval, but such an observation has not been made. *Siphonichnus* producers of different ages and potentially belonging to different species can inhabit the same interval, and this is manifested in the co-occurrence of *Siphonichnus* of different sizes. Therefore, it is not suitable to use only size to differentiate *Siphonichnus* traces in more detail. However, the distinction of morphological groups by using burrow width w_b in relation to width of the siphonal lumen w_s is suitable because it is an anatomically based measure not affected by the age/size of the producer. The two groups found appear to represent recurrent producer types because the studied *Siphonichnus* specimens display similar w_b:w_s ratios to traces figured in literature, for instance, 2–3.5 and ~ 6 (Gerard and Bromley, 2008, p. 34), 2–3.5 (Knaust, 2017, fig. 5.140b, 5.141a), and 2.5–3.5 and 4 (Stanistreet et al., 1980, fig. 14).

In many instances, the composition of the muddy host sediment clearly differs from the material constituting the mantle of mainly downward *Siphonichnus* that consists of coarse silt and fine sand

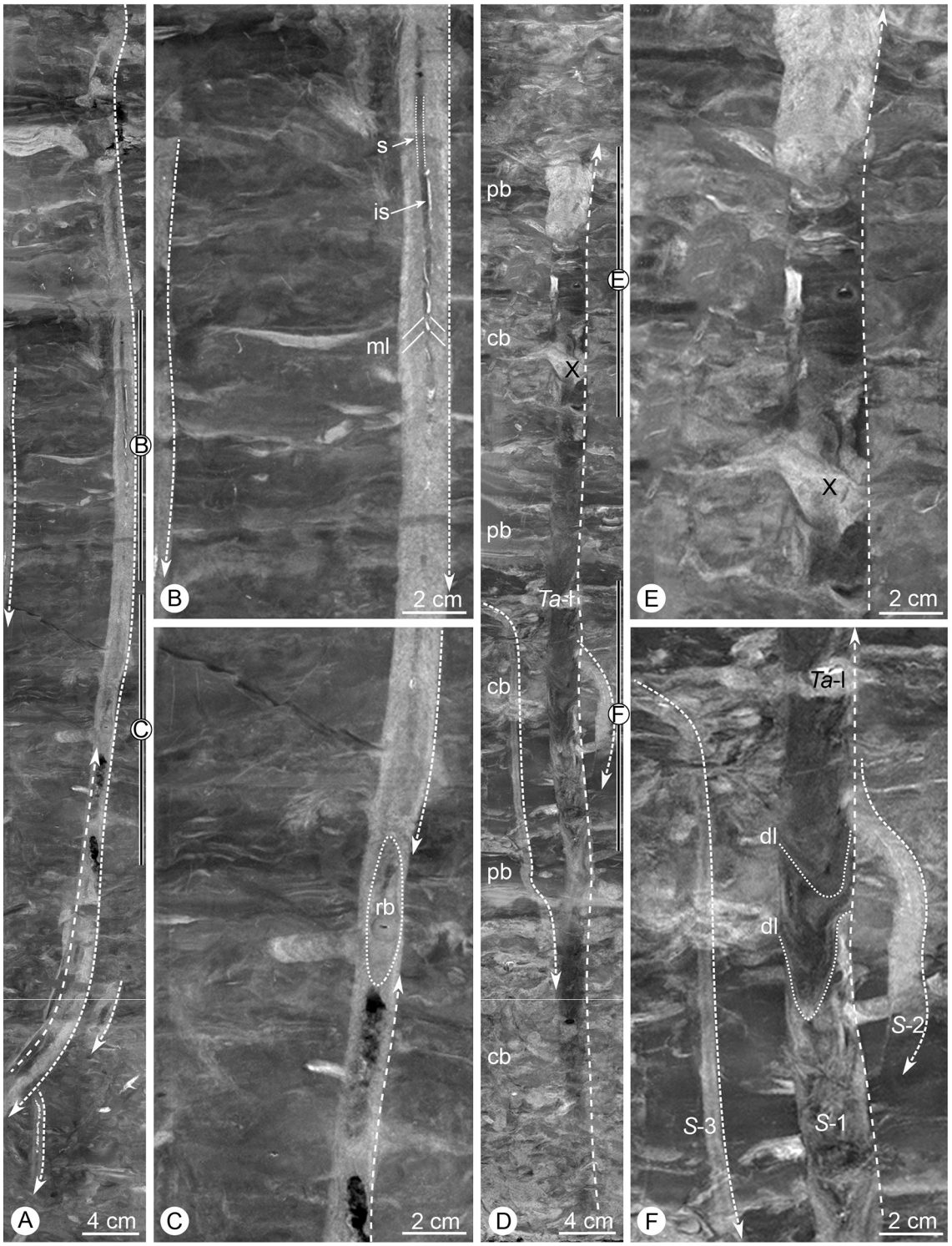

Fig. 10. *Siphonichnus* recording exceptional erosion and deposition (X-ray radiograph negatives; mud – dark, sand – light). (A) Core 28–4, 278–380 cm, traces showing downward and upward movement of the producers (indicated by arrows); during upward movement producer followed its own trace typical of a sequorichnial behavior. Black solid lines at the right mark parts shown in detail in (B) and (C). (B) Core 28–4, 300–319 cm, inclined mantle lamellae (ml) typical of downward movement of the producer (as indicated by arrow) in response to erosion; is = iron sulfide precipitated along the supposed mucous lining of the siphonal lumen (s) later filled by uniform mud; ratio of burrow width to lumen width ~ 9. (C) Core 28–4, 320–339 cm; transition from downward to upward movement (indicated by arrows), stippled line supposed place of producer (rb); note collapsed chaotic fill below producer. (D) Core 28–4, 384–476 cm, upward and downward *Siphonichnus* specimens co-occur (indicated by arrows), both disappear from plane of observation due to undulating course; completely (cb) and partly bioturbated (pb) host sediment intervals alternate; cross-cutting of *S.* by other traces (x – unidentified; *Ta*-l – *Taenidium*-like) indicate generally deep bioturbation (> 20–30 cm). Solid black lines at the right mark parts shown in detail in (E) and (F). (E) Core 28–4, 396–415 cm; upward movement of *S*. producer indicated by 'disorganized' backfill; note cross-cutting by unidentified burrow (x). (F) Core 28–4, 425–444 cm *Siphonichnus* (*S*-1) showing backfill typical of rapid upward movement of the producer in response to deposition as indicated by the fluidized appearance of deformed laminae (some marked by stippled lines dl); *S*-1 is cross-cut by *Taenidium*-like trace (*Ta*-l) produced in at least 30 cm depth; small downward *Siphonichnus* (*S*-2, *S*-3) exhibiting a ratio of burrow width to width of lumen ~3 for *S*-3.

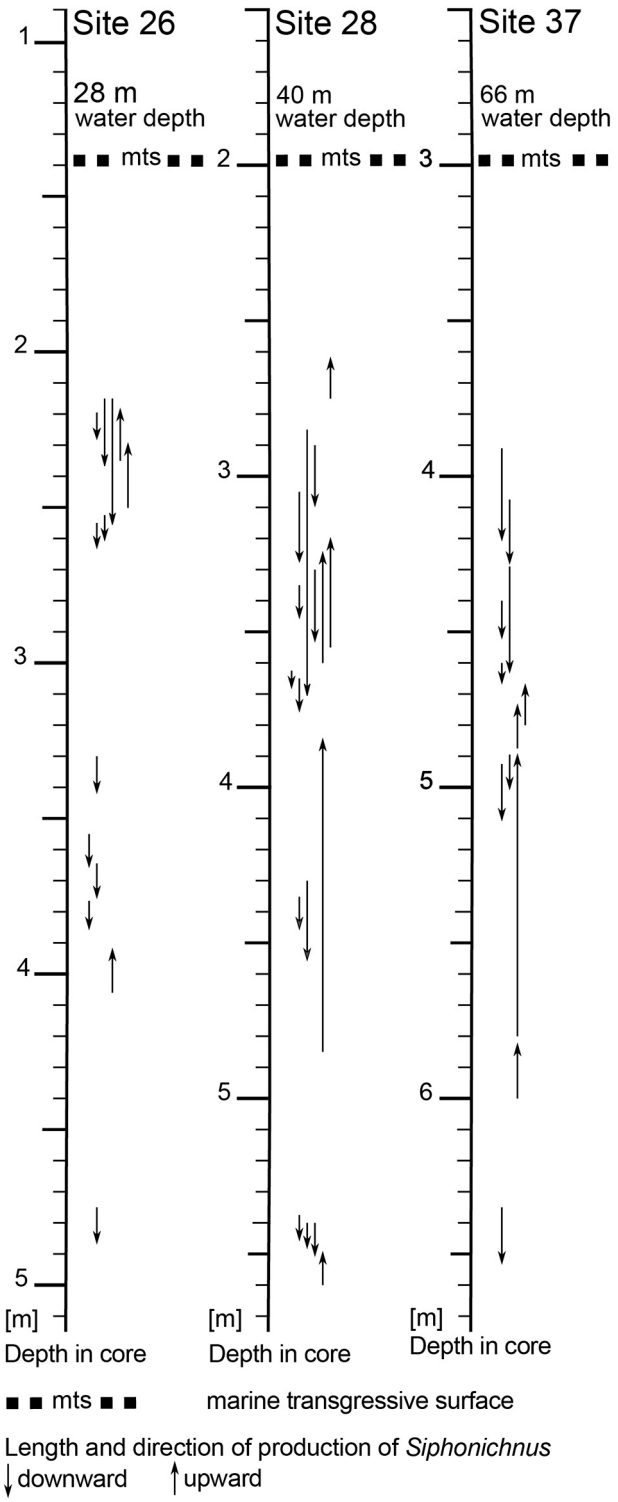

Fig. 11. *Siphonichnus* showing recurrent down- and upward movements encountered in core 26–5 (28 m water depth), 28–4 (40 m water depth), and 37–5 (66 m water depth); for location of cores see Fig. 2. The marine transgressive surface (mts = base of LF 4) was used as reference level. *Siphonichnus* occurs mainly in estuarine deposits of the FMTZ. Each arrow indicates direction of movement recorded by an individual *Siphonichnus* trace.

(Figs. 7, 10). The rather sharp burrow boundary implies a fairly cohesive host sediment. It does not display distinct compressional features around the burrow (Fig. 7A) and thus, the producers may have compacted the sediment around them only little when opening their shells. Therefore, the producers need first to excavate the sediment by transferring material along their body and partly out of the burrow, to move downward and concomitantly they convey some coarse silt and fine sand downward to construct the convex mantle menisci. The producers can resuspend mud and pump it out with respiration water to the surface. The fill material supposedly originates from the sediment surface or the bottom water. In fact, many bivalves living subsurface in stationary burrows feed from suspension or the sediment surface and have little need to change location for nutrition (Stanley, 1970). In particular, when coarser particles are available, presumably during a period of enhanced current velocity, they are taken from or above the surface to reduce the risk of clogging the gills. Also, fossil *Siphonichnus* shown in literature differ in their fill from the host sediment and illustrate that the here outlined observations do not represent singularities (e.g., Knaust, 2015). Traces occurring within muddy host sediment and containing rather pure sand were, for example, figured by Gerard and Bromley (2008, p. 34) and Knaust (2017, fig. 5.140b). The uniform fill of the siphonal lumen and the occasionally present Fe-sulfides suggest a mucus lining and passive fill because after fill of the lumen, in an anoxic micro-environment organic-rich material attracts sulfate-reducing microbes (e.g., Rickard and Luther, 2007). Fe-sulfides can only form if water containing considerable amounts of sulfate, such as seawater, is present in the tube since river water contains too little sulfate (e.g., Open University Course Team, 1995).

Living deep within sediment has been interpreted to lower the effects of salinity fluctuations, which become attenuated with depth (Knox, 1986). This hypothesis, however, is highly unlikely for burrowing bivalves because they take their respiration from above the sediment surface. Therefore, deep burrowing very likely represents an adaptation to reduce the risk of predation and of erosion as well.

The upward burrow segments overlapping downward ones document a sequorichnial behavior, because an organism followed its own trace (Nara and Seike, 2019). Furthermore, the *Siphonichnus* producers have equilibrichnial capabilities (e.g., Reineck, 1958; Stanistreet et al., 1980). The downward burrow extent minus living depth provides a minimum estimate of erosion, whereas upward movement records deposition. The increasing inclination of a burrow distally may represent a strategy to be prepared for depositional events, because it requires less energy to move horizontally than to burrow upward and to maintain an open connection to the surface. It can speculated that the extent of the horizontal burrow segment could represent an adaptation to a specific environment, which commonly experiences depositional events of a particular thickness. Furthermore, the producer stays within an interval of suitable sediment properties, and pumping of respiration water requires less energy compared to a vertical burrow of the same length. Unfortunately, the length of the inclined burrow part could not be measured directly because of small core diameter, but it definitely exceeds 10–20 cm (Fig. 7). Because of the finite length of the siphon and similar organs, rapid response to deposition is essential. The comparatively chaotic, disorganized fill structures formed during upward movement imply that water-saturated material was rather rapidly displaced downward around the body and the previously sharp burrow boundary became partly reworked (Figs. 7, 10). In case of a bivalve producer, the foot might form the tongue-like depression in the center. Solely downward burrows may indicate that during the life time of a *Siphonichnus* producer there was no need to move upward and hence, no considerable deposition took place.

The extensive downward or upward movements of the *Siphonichnus* producers document short-term erosion or deposition of > 0.5 m that is otherwise not recorded because the deposits are completely bioturbated. Only in sediments of LF2 and LF2/3, the laminated intervals record (event) deposition being commonly in the range of up to a few centimeters (Figs. 4, 7A). In contrast, the amount of erosion can only be estimated from the downward *Siphonichnus*. Vertical movements of 40–60 cm implying pronounced depositional and erosional phases recurred throughout the incised valley mainly during the estuarine stage (Fig. 11). These phases are very likely related to freshets (erosion) and

their waning stages (deposition) as observed today (cf. La Croix and Dashtgard, 2014). Depositional events may result from migrating bedforms, fluid-mud carpets, or sediment sheets moving during freshets. In any event, *Siphonichnus* illustrates that deposition was rather discontinuous. The strata filling the incised valley represent a pile of stacked depositional events interrupted by erosional phases and both deposition and erosion might have varied strongly. Unfortunately, the recurrence time of exceptional events displacing the sediment surface vertically by > 0.5 m can hardly be estimated, but it could be in the range of several hundreds of years.

Siphonichnus producers moved a maximum of 80–90 cm downward and upward in relatively tranquil valley domains. In contrast, *Siphonichnus* are absent in deposits at channel bends. The reason for that is unknown, it can only be speculated that there, during a freshet, sediment erosion and thereafter, accumulation was too high and/or too rapid to be compensated for by the burrowing capabilities of the *Siphonichnus* producers. Thus, dynamic sediment bars might have represented a habitat not suitable for *Siphonichnus* producers. This deduction is supported by the presence of *Siphonichnus* in point bar deposits of modern meandering channels that are not affected by such severe erosion and deposition (Pearson and Gingras, 2006).

6. Discussion

During times of lowered sea level, purely fluvial segments of the valley incised by the Red River in the Gulf of Tonkin were potentially in an erosional or bypass mode due to geomorphic disequilibrium (see above). Only lag deposits formed, and they provide no detailed information about the sediment dynamics. Downstream towards the river mouth, where tidal currents and fluvial discharge interact, the environment becomes increasingly dynamic. The strength of tidal currents varies significantly, as during the wet season the runoff of the Red River commonly increases by > 10 times. Temporarily seawater incurred as indicated by the presence of early diagenetic iron sulfides and the trace *Artichnus* (Fig. 10) that may occur at salinities as low as 15 PSU (see above). It has to be considered, however, that *Artichnus* can not only be produced by holothurians, also sipunculids have been found within burrows exhibiting the same characteristics (Jumars et al., 1990). These organisms can burrow deep into the sediment > 20–30 cm (Jumars et al., 1990) and some deep-burrowing species live in salinities as low as 15 PSU (e.g., Edmonds, 2000). Although burrowing bivalves may occur in settings experiencing mesohaline and higher salinities within the FMTZ (e.g., Johnson and Dashtgard, 2014), at low salinities (mesohaline and lower) they become sparse to absent (Howard et al., 1975). However, also turbidity and sediment dynamics affect the bivalves burrowing in FMTZ deposits, but a study taking into account all these factors has not yet been accomplished to our knowledge. Nonetheless, the presence of iron sulfides in the core of *Siphonichnus*, the co-occurrence with *Artichnus,* and the fact that *Siphonichnus* very likely originated from completely bioturbated intervals, but definitely occurs below the marine transgressive surface suggests that the *Siphonichnus* was produced under polyhaline conditions.

In valley segments located downstream from the backwater limit, *Siphonichnus* exhibits pronounced vertical movements > 30–50 cm, although occasionally intercalated, partly laminated intervals record deposition of only < 10 cm per event. Within the tidal limit, marine incursions, tidal currents, and freshets cause a highly dynamic environment; in particular below the contact between freshwater and seawater wedge a fluid-mud carpet may form. *Siphonichnus* and other deep burrows document a rather dynamic depositional setting although the sediments experienced complete bioturbation that is – erroneously – suggestive of a rather continuous sediment aggradation. However, complete bioturbation only indicates that the time between successive events was sufficiently long to bioturbate the deposits (e.g., Reineck, 1977) and that the endobenthic fauna was adapted to a wide grain-size spectrum to burrow both fine and coarse intervals of event layers (e.g., Wetzel, 1991). Because within the FMTZ primary production is enhanced (e.g., Cloern et al., 2014), ample supply of benthic food fueled the burrowing fauna. Consequently, complete bioturbation and the recorded clusters of *Siphonichnus* imply an estimated time between exceptional events in the range of several hundreds of years.

Due to rapid landward coastline migration the valley segment occupied by the FMTZ is potentially in disequilibrium and, therefore, the sediment record is expected to be rather incomplete and dominated by short-term depositional and erosional phases. In fact, the estuarine Holocene sediment pile consists of stacked event beds, but the original record was subsequently extinguished by intense bioturbation. Severe erosional and depositional events are recorded only by *Siphonichnus*. In addition, the large proportion of deep-burrowing organisms that crosscut deep parts of *Siphonichnus* characterizes an environment experiencing occasionally severe erosion. These burrows, however, provide only a rough estimate of the sediment dynamics with respect to timing because the previous sediment surface from which the burrows originated is unknown due to recurrent erosion and deposition and subsequent bioturbation. Exceptional vertical movements of bivalves are also known from similar settings in the rock record. In the Devonian Catskill river mouth deposits, bivalves moved for ~1 m vertically (Knoll et al., 2017).

The established concepts of bivalve burrowing techniques (see Stanley, 1970) do not apply for the sandy fill of *Siphonichnus* that resulted from downward burrowing and subsequent filling by material differing from the adjacent host sediment. As no organisms other than bivalves have been found yet that produce *Siphonichnus*, further studies and observations on *Siphonichnus* and potential producers are needed to better understand this particular aspect of their fill.

7. Conclusions

Rapid sea-level changes affected the low-gradient shelf and the coastal region of the Gulf of Tonkin: Sea-level fall was so fast that the valley system traversing the present Gulf of Tonkin did not reach geomorphic equilibrium and remained prone to erosion. In contrast, during Holocene sea-level rise, coastline migration of, on average, ~60 m yr^{-1} was too rapid to facilitate development of sand bars and barriers within the river mouth and, therefore, the river mouth represented an open, funnel-shaped muddy estuary.

During the Holocene sea-level rise, the valley incised by the Red River into the Gulf of Tonkin was in a net aggrading mode. In particular, completely bioturbated sediments suggest – erroneously – fairly continuous deposition, whereas only partly bioturbated deposits at the base of the estuarine deposits document depositional events up to 10 cm and some erosion that, however, cannot be estimated. These events could be related to seasonal events like freshets, with ~10 cm of erosion and deposition.

Further up, in strongly bioturbated deposits containing some iron sulfides, pronounced, > 60–80 cm downward and upward movements of the *Siphonichnus* producers imply predominantly discontinuous sediment accumulation. Depositional and erosional events exceeding 60–80 cm recurred as long as a valley segment experienced polyhaline conditions and as it was located between the backwater limit and the open sea, the latter indicated by remains of a fully marine fauna. These exceptional events leading to > 60–80 cm erosion and/or subsequent deposition may have had a recurrence time in the range of several hundreds of years.

In fact, the estuarine Holocene sediment pile consists of stacked event beds, but the original record was subsequently extinguished by intense bioturbation. Severe erosional and depositional events are only recorded by *Siphonichnus*.

Declaration of Competing Interest

The authors declare that they have no known competing financial interests or personal relationships that could have appeared to influence the work reported in this paper.

Acknowledgements

RV *Sonne* cruise 220 was funded by the German Ministry of Science and Education (grant no. 03G0220B). The chief scientists Karl Stattegger (Kiel, Germany) and Martin Wiesner (Hamburg, Germany) graciously provided access to the core material and contributed valuable background information. Fruitful conversations with D. Knaust (Stavanger, Norway) provided additional insights to better understand *Siphonichnus*. The Radiology section of the Medical Care Center (Prüner Gang) in Kiel (Germany) generously provided access to their equipment to obtain X-ray radiographs. Constructive reviews by S. Dashtgard (Burnaby, Canada) and A. Rindsberg (Livingston, Alabama, U.S.A.) helped to improve the manuscript. A.W. received funds from the Swiss National Foundation (SNF grant no. 200020_140217/1). D.U. was financially supported by the German Science Foundation (grant no. STA 401-10 to Karl Stattegger, Kiel). All these contributions are gratefully acknowledged.

References

Aller, R.C., 1994. Bioturbation and remineralization of sedimentary organic matter: effects of redox oscillation. Org. Geochem. 114, 331–345.
Ayranci, K., Dashtgard, S.E., MacEachern, J.A., 2014. A quantitative assessment of the neoichnology and biology of a delta front and prodelta, and implications for delta ichnology. Palaeogeogr. Palaeoclimatol. Palaeoecol. 409, 114–134.
Azhikodan, G., Yokoyama, K., 2018. Sediment transport and fluid mud layer formation in the macro-tidal Chikugo river estuary during a fortnightly tidal cycle. Estuar. Coast. Shelf Sci. 202, 232–245.
Bertling, M., Braddy, S.J., Bromley, R.G., Demathieu, G.R., Genise, J., Mikulas, R., Nielsen, J.K., Nielsen, K.S.S., Rindsberg, A.K., Schlirf, M., Uchman, A., 2006. Names for trace fossils: a uniform approach. Lethaia 39, 265–286.
Blum, M., Martin, J., Milliken, K., Garvin, M., 2013. Paleovalley systems: Insights from Quaternary analogs and experiments. Earth Sci. Rev. 116, 128–169.
Borges, J., Huh, Y., 2007. Petrography and chemistry of the bed sediments of the Red River in China and Vietnam: Provenance and chemical weathering. Sediment. Geol. 194, 155–168.
Boyd, R., Dalrymple, R.W., Zaitlin, B.A., 2006. Estuary and incised valley facies models. In: Posamentier, H.W., Walker, R.G. (Eds.), Facies Models Revisited. Special Publication 84. pp. 171–234.
Bromley, R.G., 1996. Trace fossils. In: Biology, Taphonomy and Applications. Chapman and Hall, London, pp. 361.
Cloern, J.E., Foster, S.Q., Kleckner, A.E., 2014. Phytoplankton primary production in the world's estuarine-coastal ecosystems. Biogeosciences 11, 2477–2501.
Dashtgard, S.E., Gingras, M.K., 2012. Marine invertebrate ichnology. In: Knaust, D., Bromley, R.G. (Eds.), Trace Fossils as Indicators of Sedimentary Environments. Developments in Sedimentology 64. Elsevier, Amsterdam, pp. 273–295.
Dashtgard, S.E., La Croix, A.D., 2015. Sedimentological trends across the tidal-fluvial transition, Fraser River, Canada: A review and some broader implications. In: P. Ashworth, J. Best, D.R. Parsons (Eds.), Fluvial-Tidal Sedimentology. Developments in Sedimentology, 68. Elsevier, Amsterdam, pp. 111–126.
Edmonds, S.J., 2000. Polychaetes & allies – The southern synthesis. 5. Phylum Sipuncula. In: Beesley, P.L., Ross, G.J.B., Glasby, C. (Eds.), Fauna of Australia. CSIRO Publishing, Melbourne, pp. 37.
Fagherazzi, S., Howard, A.D., Wiberg, P.L., 2004. Modeling fluvial erosion and deposition on continental shelves during sea level cyclces. J. Geophys. Res. 109 (F03010), 1–16.
Franz, G., Pinto, L., Ascione, I., Mateus, M., Fernandes, R., Leitão, P., Neves, R., 2014. Modelling of cohesive sediment dynamics in tidal estuarine systems: Case study of Tagus estuary, Portugal. Estuar. Coast. Shelf Sci. 151, 34–44.
Gerard, J., Bromley, R., 2008. Ichnofabrics in Clastic Sediments. Jean R.F. Gerard, Madrid, pp. 100.
Gingras, M.K., MacEachern, J.A., Dashtgard, S.E., Zonneveld, J.-P., Schoengut, J., Ranger, M.J., Pemberton, S.G., 2012. Estuaries. In: Knaust, D., Bromley, R.G. (Eds.), Trace Fossils as Indicators of Sedimentary Environments. Developments in Sedimentology, vol. 64. Elsevier, Amsterdam, pp. 463–505.
Goldring, R., 1995. Organisms and the substrate: response and effect. In: Bosence, D.J.W., Allison, P.A. (Eds.), Marine Palaeoenvironmental Analysis from Fossils. Geological Society of London, Special Publication 83. pp. 151–180.
Gugliotta, M., Saito, Y., Nguyen, V.L., Ta, T.K.O., Nakashima, R., Tamura, T., Uehara, K., Katsuki, K., Yamamoto, S., 2017. Process regime, salinity, morphological, and sedimentary trends along the fluvial to marine transition zone of the mixed-energy Mekong River delta, Vietnam. Cont. Shelf Res. 147, 7–26.
Hanebuth, T.J.J., Stattegger, K., 2003. The stratigraphic evolution of the Sunda Shelf during the past fifty thousand years. In: Sidi, F.H., Nummedal, D., Imbert, P., Darman, H., Posamentier, H.W. (Eds.), Tropical Deltas of Southeast Asia – Sedimentology, Stratigraphy, and Petroleum Geology. SEPM (Society for Sedimentary Geology) Special Publication 76. pp. 189–200.
Hanebuth, T.J.J., Stattegger, K., Bojanowski, A., 2009. Termination of the Last Glacial Maximum sea-level lowstand: The Sunda-Shelf data revisited. Glob. Planet. Chang. 66, 76–84.
Haruyama, S., 1995. Geomorphic environment of Tonkin delta. In: The Study of International Relations, Tsuda College. 21. pp. 1–13 (in Japanese).
Hertweck, G., 1972. Distribution and environmental significance of lebensspuren and in situ skeletal remains. Senckenberg. Marit. 4, 125–167.
Howard, J.D., Frey, R.W., 1975. Regional animal-sediment characteristics of Georgia estuaries. Senckenberg. Marit. 7, 33–107.
Howard, J.D., Elders, C.A., Heinbokel, J.F., 1975. Animal-relationships in estuarine point bar deposits, Ogeechee River-Ossabaw Sound, Georgia. Senckenberg. Marit. 7, 181–203.
Johnson, S.M., Dashtgard, S.E., 2014. Inclined heterolithic stratification in a mixed-tidal-fluvial channel: Differentiating tidal versus fluvial controls on sedimentation. Sediment. Geol. 301, 41–53.
Jumars, P., Mayer, L.M., Deming, J.W., Baross, J., Wheatcroft, R.A., 1990. Deep-sea deposit-feeding strategies suggested by environmental and feeding constraints. Phil. Trans. R. Soc. Lond., A 331, 85–101.
Knaust, D., 2012. Trace fossil systematics. In: Knaust, D., Bromley, R.G. (Eds.), Trace Fossils as Indicators of Sedimentary Environments. Developments in Sedimentology, vol. 64. Elsevier, Amsterdam, pp. 79–101.
Knaust, D., 2015. Siphonichnidae (new ichnofamily) attributed to the burrowing activity of bivalves: Ichnotaxonomy, behaviour and palaeoenvironmental implications. Earth Sci. Rev. 150, 497–519.
Knaust, D., 2017. Atlas of Trace Fossils in Well Core. Springer, Cham, pp. 209.
Knoll, K., Chamberlain, R.B., Chamberlain, J.A., 2017. Escape burrowing of modern freshwater bivalves as a paradigm for escape behavior in the Devonian bivalve *Archanodon catskillensis*. Geosciences 7 (102), 1–37.
Knox, G.A., 1986. Estuarine Ecosystems: A Systems Approach (Volume I). CRC Press, Boca Raton, pp. 289.
Kranz, P.M., 1974. The anastrophic burial of bivalves and its paleoecological significance. J. Geol. 82, 237–265.
La Croix, A.D., Dashtgard, S.E., 2014. Of sand and mud: Sedimentological criteria for identifying the turbidity maximum zone in a tidally influenced river. Sedimentology 62, 1961–1981.
La Croix, A.D., Dashtgard, S.E., 2015. A synthesis of depositional trends in intertidal and upper subtidal sediments across the tidal-fluvial transition in the Fraser River, Canada. J. Sediment. Res. 85, 683–698.
La Croix, A.D., Dashtgard, S.E., Gingras, M.K., Hauck, T.E., MacEachern, J.A., 2015. Bioturbation trends across the freshwater to brackish transition. Palaeogeogr. Palaeoclimatol. Palaeoecol. 440, 66–77.
Liu, Z.F., Zhao, Y.L., Ri, J.R., Colin, C., 2007. Late Quaternary clay minerals off Middle Vietnam in the western South China Sea: Implications for source analysis and East Asian monsoon evolution. Sci. China Ser. D Earth Sci. 50, 1674–1684.
Mathers, S., Zalasiewicz, J., 1999. Holocene sedimentary architecture of the Red River Delta, Vietnam. J. Coast. Res. 15, 314–325.
Mattheus, C.R., Rodriguez, A.B., 2011. Controls on Late Quaternary incised-valley dimension along passive margins evaluated using empirical data. Sedimentology 58, 1113–1137.
Moss, D.K., Ivany, L.C., Judd, E.J., Cummings, P.W., Bearden, C.E., Kim, W.-J., Artuc, E.G., Driscoll, J.R., 2016. Lifespan, growth rate, and body size across latitude in marine Bivalvia, with implications for Phanerozoic evolution. Proc. R. Soc. B 283, 7 20161364.
Nara, M., Seike, K., 2019. Palaeoecology of *Macaronichnus segregatis degiberti*: Reconstructing the infaunal lives of the travisiid polychaetes. Palaeogeogr. Palaeoclimatol. Palaeoecol. 516, 284–294.
Open University Course Team, 1995. Seawater: Its Composition, Properties and Behaviour, 2nd ed. Butterworth-Heinemann, Oxford, pp. 168.
Pearson, N.J., Gingras, M.K., 2006. An ichnological and sedimentological facies model for muddy point-bar deposits. J. Sediment. Res. 76, 771–782.
Postma, D., 1982. Pyrite and siderite formation in brackish and freshwater swamp sediments. Am. J. Sci. 282, 1151–1183.
Reineck, H.-E., 1958. Wühlbau-Gefüge in Abhängigkeit von der Sediment-Umlagerung. Senckenb. Lethaea 39, 1–23.
Reineck, H.-E., 1977. Natural indicators of energy level in recent sediments: The application of ichnology to a coastal engineering problem. In: Crimes, T.P., Harper, J.C. (Eds.), Trace Fossils 2. Geological Journal Special Issue, vol. 9. Seel House Press, Liverpool, pp. 265–272.
Rickard, D., Luther, G.W.I., 2007. Chemistry of iron sulfides. Chem. Rev. 107, 514–562.
Schimanski, A., Stattegger, K., 2005. Deglacial and Holocene evolution of the Vietnam shelf: Stratigraphy, sediments and sea-level change. Mar. Geol. 214, 365–387.
Schumm, S.A., 1993. River response to base level change: Implications for sequence stratigraphy. J. Geol. 101, 279–294.
Stanistreet, I.G., Le Blanc Smith, G., Cable, A.B., 1980. Trace fossils as sedimentological and palaeoenvironmental indices in the Ecca Group (Lower Permian) of Transvaal. Trans. Geol. Soc. South Afr. 83, 333–344.
Stanley, S.M., 1970. Relation of shell form to life habits in the Bivalvia (Mollusca). Geol. Soc. Am. Mem. 125, 296.
Stattegger, K., Tjallingii, R., Saito, Y., Michelli, M., Trung Thanh, N., Wetzel, A., 2013. Mid- to late Holocene sea-level reconstruction of Southeast Vietnam using beachrock and beach-ridge deposits. Glob. Planet. Change 110, 214–222.

Szczuciński, W., Jagodziński, R., Hanebuth, T.J.J., Stattegger, K., Wetzel, A., Mitręga, M., Unverricht, D., Van Phach, P., 2013. Modern sedimentation and sediment dispersal pattern on the continental shelf off the Mekong River delta, South China Sea. Glob. Planet. Change 110, 195–213.

Tanabe, S., Saito, Y., Vu, Q.L., Hanebuth, T.J.J., Ngo, Q.L., Kitamura, A., 2006. Holocene evolution of the Song Hong (Red River) delta system, northern Vietnam. Sediment. Geol. 187, 29–61.

Tjallingii, R., Stattegger, K., Wetzel, A., Van Pach, P., 2010. Infilling and flooding of the Mekong River incised-valley system during deglacial sea-level rise. Quat. Sci. Rev. 29, 1432–1444.

Tomczak, M., Godfrey, J.S., 1994. Regional Oceanography. Pergamon, London, pp. 422.

van Maren, D.S., 2007. Water and sediment dynamics in the Red River mouth and adjacent coastal zone. J. Asian Earth Sci. 29, 508–522.

Voris, H.K., 2000. Maps of Pleistocene sea levels in Southeast Asia: Shorelines, river systems and time durations. J. Biogeogr. 27, 1153–1167.

Wang, P., Li, Q., 2009. The South China Sea. Paleoceanography and sedimentology. In: Developments in Paleoenvironmental Research. 13. Springer, Berlin, Heidelberg, New York, pp. 506.

Wang, L., Sarnthein, M., Erlenkeuser, H., Grimalt, J., Grootes, P., Heilig, S., Ivanova, E., Kienast, M., Pelejero, C., Pflaumann, U., 1999. East Asian monsoon climate during the Late Pleistocene: High-resolution sediment records from the South China Sea. Mar. Geol. 156, 245–284.

Werner, F., 1967. Röntgen-Radiographie zur Untersuchung von Sedimentstrukturen. Umschau 16, 532.

Wetzel, A., 1981. Ökologische und stratigraphische Bedeutung biogener Gefüge in quartären Sedimenten am NW-afrikanischen Kontinentalrand. "Meteor" Forschungs-Ergebnisse, Reihe C 34, 1–47.

Wetzel, A., 1991. Ecologic interpretation of deep-sea trace fossil communities. Palaeogeogr. Palaeoclimatol. Palaeoecol. 85, 47–69.

Wetzel, A., 2010. Deep-sea ichnology: Observations in modern sediments to interpret fossil counterparts. Acta Geol. Pol. 60, 125–138.

Wetzel, A., Werner, F., 1981. Morphology and ecological significance of *Zoophycos* in deep-sea sediments off NW Africa. Palaeogeogr. Palaeoclimatol. Palaeoecol. 32, 185–212.

Wetzel, A., Szczygielski, A., Unverricht, D., Stattegger, K., 2017. Sedimentological and ichnological implications of rapid Holocene flooding of a gently sloping mud-dominated incised valley – an example from the Red River (Gulf of Tonkin). Sedimentology 64, 1173–1202.

Wiesner, M.G., Stattegger, K., Pohlmann, T., Chen, F., Heddaeus, A., Heyckendorff, K., Jechlitschek, H., Lahajnar, N., Liskow, I., Li, X., Liu, Z., Lorenc, S., Metzke, M., Müller, M., Peleo-Alampay, A., Schönke, M., Schwarzer, K., Szczygielski, A., Steen, E., Unverricht, D., Wang, X., Welsch, A., Wetzel, A., Zhao, Y., 2012. Cruise Report RV *Sonne* 220 – Land-Ocean-Atmosphere Interactions in the Gulf of Tonkin. Institut für Geowissenschaften Universität Kiel, pp. 101.

Zaitlin, B.A., Dalrymple, R.W., Boyd, R., 1994. The stratigraphic organization of incised-valley systems associated with relative sea-level change. In: Dalrymple, R.W., Zaitlin, B.A., Scholle, P.A. (Eds.), Incised-Valley Systems: Origin and Sedimentary Sequences. SEPM (Society for Sedimentary Geology) Special Publication 51. pp. 45–60.